ASTROCHEMISTRY

Detection of interstellar 1-cyanopyrene: A four-ring polycyclic aromatic hydrocarbon

Gabi Wenzel[1]*, Ilsa R. Cooke[2]*, P. Bryan Changala[3], Edwin A. Bergin[4], Shuo Zhang[1], Andrew M. Burkhardt[5], Alex N. Byrne[1], Steven B. Charnley[6], Martin A. Cordiner[6], Miya Duffy[1], Zachary T. P. Fried[1], Harshal Gupta[3,7], Martin S. Holdren[1], Andrew Lipnicky[8], Ryan A. Loomis[8], Hannah Toru Shay[1], Christopher N. Shingledecker[9], Mark A. Siebert[10]†, D. Archie Stewart[1], Reace H. J. Willis[2], Ci Xue[1], Anthony J. Remijan[8], Alison E. Wendlandt[1], Michael C. McCarthy[3], Brett A. McGuire[1,8]*

Polycyclic aromatic hydrocarbons (PAHs) are organic molecules containing adjacent aromatic rings. Infrared emission bands show that PAHs are abundant in space, but only a few specific PAHs have been detected in the interstellar medium. We detected 1-cyanopyrene, a cyano-substituted derivative of the related four-ring PAH pyrene, in radio observations of the dense cloud TMC-1, using the Green Bank Telescope. The measured column density of 1-cyanopyrene is ~1.52 × 10^{12} cm^{-2}, from which we estimate that pyrene contains up to 0.1% of the carbon in TMC-1. This abundance indicates that interstellar PAH chemistry favors the production of pyrene. We suggest that some of the carbon supplied to young planetary systems is carried by PAHs that originate in cold molecular clouds.

The infrared spectra of many dust-rich astronomical objects are dominated by a set of emission bands, historically known as the unidentified infrared (UIR) bands (*1*). Despite the name, the carriers of the UIR bands are widely accepted to be polycyclic aromatic hydrocarbons (PAHs), a class of organic molecules (*2*, *3*). The UIR bands have been observed in objects at many stages of the stellar life cycle, specifically in regions illuminated by hot stars or the interstellar radiation field, which are called photon-dominated regions (PDRs). The UIR bands have been assigned to vibrational modes of large PAHs (those with ≳35 carbon atoms) whose stability to ultraviolet (UV) radiation means that they are expected to survive even under harsh interstellar conditions (*4*). Although the UIR bands do not identify specific PAH molecules, they demonstrate that PAHs are ubiquitous organic compounds in space. The intensity of the UIR bands indicates that ~10 to 25% of all carbon in the interstellar medium (ISM) of the Milky Way is incorporated into PAHs (*1*, *4*, *5*, *6*).

[1]Department of Chemistry, Massachusetts Institute of Technology, Cambridge, MA 02139, USA. [2]Department of Chemistry, University of British Columbia, Vancouver, BC V6T 1Z1, Canada. [3]Center for Astrophysics, Harvard & Smithsonian, Cambridge, MA 02138, USA. [4]Department of Astronomy, University of Michigan, Ann Arbor, MI 48109, USA. [5]Department of Earth, Environment, and Physics, Worcester State University, Worcester, MA 01602, USA. [6]Astrochemistry Laboratory, NASA Goddard Space Flight Center, Greenbelt, MD 20771, USA. [7]Division of Astronomical Sciences, National Science Foundation, Alexandria, VA 22314, USA. [8]National Radio Astronomy Observatory, Charlottesville, VA 22903, USA. [9]Department of Chemistry, Virginia Military Institute, Lexington, VA 24450, USA. [10]Department of Astronomy, University of Virginia, Charlottesville, VA 22904, USA.
***Corresponding author. Email: gwenzel@mit.edu (G.W.); icooke@chem.ubc.ca (I.R.C.); brettmc@mit.edu (B.A.M.)**
†Present address: Department of Space, Earth and Environment, Chalmers University of Technology, SE-412 96 Gothenburg, Sweden.

PAHs are also present in meteorites classified as carbonaceous chondrites, which are material left over from the formation of the Solar System (*7*). They have also been found in samples collected from comets (*8*) and asteroids (*9*). Laboratory isotopic analysis of asteroid PAHs has shown that at least some of them formed in the cold ISM (*10*). Potential formation mechanisms include kinetically controlled mass growth processes, where the rate of formation determines the products that form (rather than the relative thermodynamic stabilities) (*11*). PAHs could alternatively form in high-temperature (~1000 K) regions, such as circumstellar envelopes around evolved stars (*12*), but it remains unclear whether PAHs are inherited from these regions into molecular clouds. Small PAHs (those with ≲35 carbon atoms) are expected to be destroyed by shock waves, cosmic rays, and UV photons faster than they can be injected from circumstellar envelopes into the ISM (*13*). Contrary to this prediction, small two-ring PAHs have been observed in the cold interstellar cloud TMC-1, which is part of the wider Taurus molecular cloud complex. These include 1- and 2-cyanonaphthalene (*14*), indene (*15*, *16*), and 2-cyanoindene (*17*). Three of those molecules contain a cyano (–CN) group attached to one of the hydrocarbon rings, which makes the molecule easier to detect with rotational spectroscopy (see below).

Pyrene is a PAH containing four aromatic rings that is particularly stable; once formed, it is difficult to destroy (*18*). This theoretical expectation is consistent with the high abundances of pyrene (relative to other PAHs) that have been measured in carbonaceous chondrites (*19*, *20*) and samples of the asteroid Ryugu (*10*). Although high-temperature routes to pyrene have been proposed (*12*), analyses of Ryugu samples indicate that pyrene formed in cold interst… environments (*10*). Some low-temperature m… anisms to form naphthalene have been proposed, but conventional chemical models have so far been unable to reproduce its inferred abundance (*21*). Quantifying pyrene in cold molecular clouds could therefore constrain low-temperature PAH formation mechanisms that impact the chemical form in which carbon is carried to subsequent stages of stellar evolution.

Searching for 1-cyanopyrene in TMC-1

We analyzed radio observations of TMC-1 with near-continuous coverage from approximately 8 to 36 GHz. The data were collected with the 100-m Robert C. Byrd Green Bank Telescope (GBT) as part of the GBT Observations of TMC-1: Hunting Aromatic Molecules (GOTHAM) project (*22*). A molecule must have a permanent electric dipole to be detected with rotational spectroscopy. Most PAHs have a small or zero dipole moment, so they cannot be readily observed with radio astronomy, but their presence can be indirectly inferred by searching for chemically related molecules. Laboratory experiments have shown that CN-functionalized aromatics can be used as efficient proxies when searching for their pure hydrocarbon counterparts that do not possess permanent dipole moments (*23*, *24*).

Pyrene is the smallest PAH in which all rings are connected to at least two others (termed compact or pericondensed). Substituting a –CN group for one of the H atoms of pyrene forms cyanopyrene ($C_{17}H_9N$), which has a large permanent electric dipole moment and is potentially observable with radio spectroscopy. Three distinct cyanopyrene isomers are possible (Fig. 1), but no published laboratory rotational spectroscopy was available for them. We performed theoretical quantum chemical calculations (*26*) of the lowest-energy isomer, 1-cyanopyrene (*25*), finding predicted permanent dipole moments of $\mu_a = 4.8$ D and $\mu_b = 2.3$ D along the *a* and *b* components of its

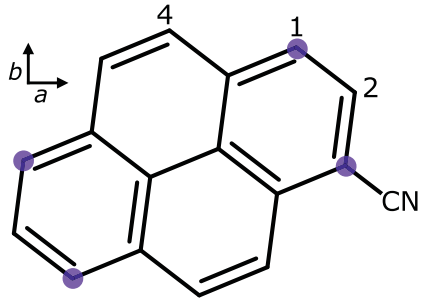

Fig. 1. Molecular structure of 1-cyanopyrene. Numbers label the carbon sites discussed in the text. Violet dots indicate equivalent substitution sites of pyrene to form the same 1-cyanopyrene isomer, which is shown on its principal axis system as indicated by the vectors *a* and *b*.

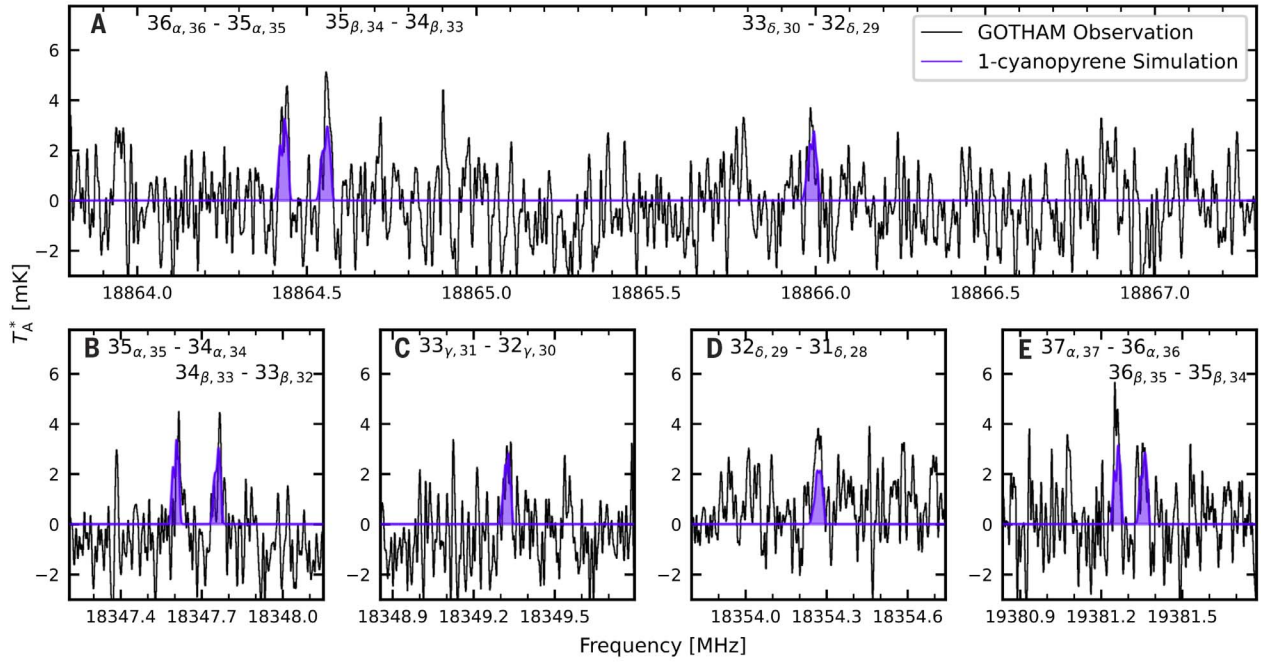

Fig. 2. 1-cyanopyrene lines detected in the TMC-1 observations. (**A** to **E**) Black lines are the GOTHAM observations, plotted as atmosphere-corrected antenna temperature (T_A^*) as a function of frequency, smoothed with a 10-channel Hanning window to a resolution of 14 kHz. Violet lines show a simulated spectrum of 1-cyanopyrene, using our derived molecular parameters (table S4). Violet shading indicates the area under the simulated spectrum. The quantum numbers of each transition, $J'_{K'_a,K'_c} - J''_{K''_a,K''_c}$, are labeled above each line (ignoring ^{14}N nuclear electric quadrupole splitting). Each line contains multiple closely spaced K_a components of each transition, which are denoted $\alpha, \beta, \gamma, \delta = \{0,1\}, \{1,2\}, \{2,3\}, \{3,4\}$.

principal axis system (Fig. 1), respectively. The calculations predicted strong rotational transitions between 8 and 22 GHz (*26*), a frequency range that overlaps with the GOTHAM dataset (*17*, *26*, *27*).

We therefore measured a laboratory rotational spectrum of 1-cyanopyrene. We synthesized 1-cyanopyrene from pyrene (*26*) (figs. S1 and S2), evaporated it in a laser ablation–supersonic expansion source, then measured its spectrum using a cavity-enhanced Fourier transform microwave spectrometer (*26*). The resulting line positions were spectroscopically assigned according to the theoretical quantum chemical predictions of the rotational constants (*26*). We measured 267 individual or partly blended rotational transitions over the 7-to-16-GHz frequency range. Their positions were fitted by using a rotational Hamiltonian, which we used to extrapolate the rest-frame transition frequencies over the entire GOTHAM frequency range with precision <2 kHz (*26*).

The transition frequencies were used to search for 1-cyanopyrene in the GOTHAM observations. Previous radio observations of TMC-1 have shown that it contains four partially overlapping velocity components (*28*). We used a Markov chain Monte Carlo (MCMC) analysis to determine the column density of 1-cyanopyrene in each velocity component (*26*). This analysis assumed tight prior probability distributions for the velocities, temperature, and linewidth

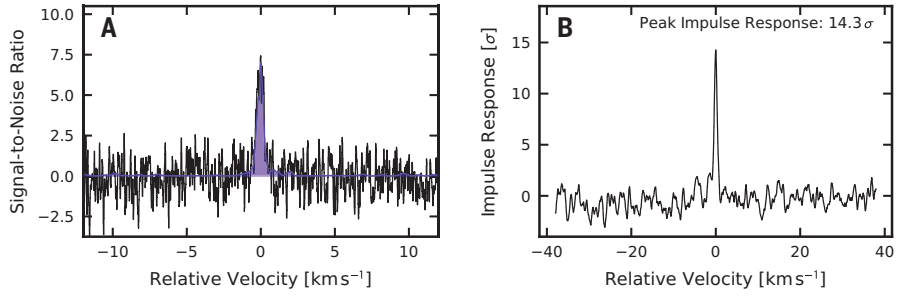

Fig. 3. Velocity-stacked spectra and matched-filter response for 1-cyanopyrene. (**A**) The GOTHAM observations stacked in velocity space (black line), relative to the systemic velocity of TMC-1, which is 5.8 km s^{-1}. The stack consists of the 150 highest S/N lines of 1-cyanopyrene and is compared with the simulated spectrum (violet line with violet shading). (**B**) The corresponding impulse response from our matched-filter analysis, which indicates that 1-cyanopyrene is detected with a significance of 14.3σ (fig. S6 shows the same data on a zoomed velocity scale).

on the basis of previous detections of PAHs (*14*) in this source (table S4). From the MCMC analysis, we derived the total column density $N(C_{17}H_9N)$ as the sum of the column densities in all four velocity components, finding $N(C_{17}H_9N) = 1.52^{+0.18}_{-0.16} \times 10^{12}$ cm^{-2} and a single excitation temperature of 7.87 K. Adopting a column density of molecular hydrogen of $N(H_2) \approx 10^{22}$ cm^{-2} from prior observations (*29*, *30*), this corresponds to an abundance ratio of $N(C_{17}H_9N)/N(H_2) \approx 1.5 \times 10^{-10}$. Figure 2 shows a simulated rotational spectrum of 1-cyanopyrene adopting our measured parameters, compared with the radio observations. Several individual lines were detected (*26*).

In addition to searching for the individual lines, we performed a velocity-stack and matched-filtering analysis to determine the total statistical evidence confirming that our model of molecular emission from 1-cyanopyrene matches the observations, following previous methods (*14*, *28*). Small spectral windows, centered around each of the 150 brightest signal-to-noise (S/N) ratio 1-cyanopyrene lines in frequency space, were extracted from the radio data and combined by using S/N weighting to

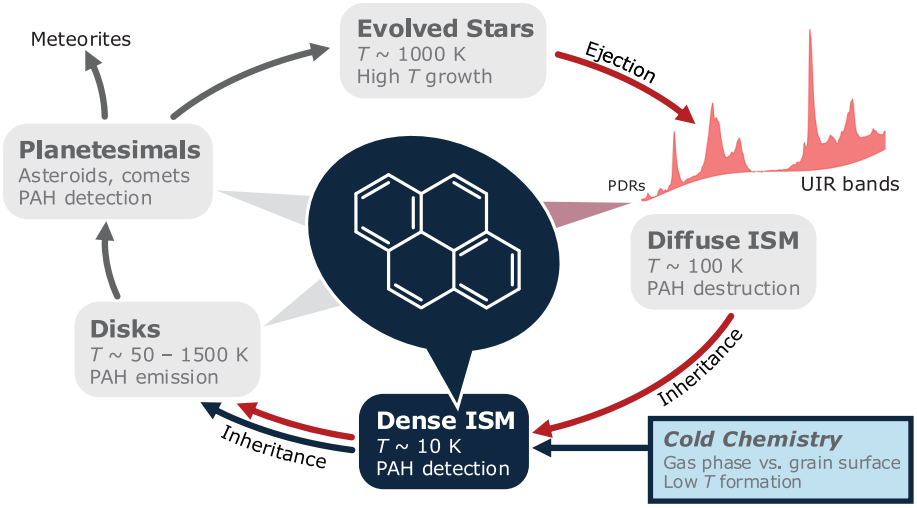

Fig. 4. Schematic illustration of PAHs in the ISM and stellar environments. Triangles extending from the central ellipse indicate locations where PAHs have been observed. PAHs form in circumstellar envelopes of evolved stars (*12*, *40*), then are ejected into the diffuse ISM (red arrows). There, PAHs are exposed to UV photons of the interstellar radiation field, producing emission of the UIR bands (*41*); theoretical models predict that this exposure destroys PAHs with <50 carbon atoms (*42*). However, we detected 1-cyanopyrene in the cold, dense ISM as a proxy for pyrene, which is invisible to radio astronomy. It is unknown whether this molecule was inherited from evolved stars (red arrows) or formed in situ through cold chemistry (blue arrows). Further processes of star and planet formation could then incorporate pyrene and other PAHs into protoplanetary disks (*43*), planetesimals (*10*), and meteorites (*7*).

produce a single average line in velocity space (Fig. 3A) (*26*). Using the stacked, simulated spectrum as a matched filter gives an impulse response of 14.3σ, indicating the total statistical significance of the detection (*28*). We performed several tests to check the robustness of the detection (*26*).

The carbon budget of TMC-1

We used the measured abundance of 1-cyanopyrene to estimate the abundance of pyrene by considering the ratio of pure hydrocarbon aromatics to their CN-substituted species, which we refer to as the H:CN ratio. On the basis of the observed H:CN ratios for other related aromatic molecules in TMC-1, we estimate the abundance of pyrene relative to H_2 as $\sim(0.15 \text{ to } 1.5) \times 10^{-8}$ (see supplementary text). Pyrene contains 16 carbon atoms, so the abundance (relative to H nuclei) of carbon atoms contained in pyrene is $(0.12 \text{ to } 1.2) \times 10^{-7}$. This corresponds to 0.007 to 0.07% of the carbon budget of TMC-1, adopting the initial elemental abundance of carbon with respect to H nuclei, $n_C/n_H = 1.8 \times 10^{-4}$ (*31*). If we instead consider the available gas-phase carbon by adopting a CO abundance in TMC-1 of 8.5×10^{-4} (relative to H) (*32*), pyrene accounts for 0.01 to 0.1% of the gas-phase carbon budget.

Supplementary table S5 compares our column densities and carbon abundances measured for 1-cyanopyrene and estimated for pyrene with other aromatic and cyclic species previously detected in TMC-1. We found that cyanopyrene has a similar abundance to the single-ring aromatic molecule benzonitrile and is more abundant than any other detected CN-substituted aromatic molecule. For comparison, the sum of the observed abundance of carbon in the cyanopolyynes (HC_mN, where m = 3 to 11) in TMC-1 is $\sim 7 \times 10^{-8}$ (*28*); thus, pyrene contains 20 to 200% of the carbon atoms that are contained in the cyanopolyynes. We suggest that the abundance of pyrene relative to other molecules in TMC-1 implies that there may be a substantial reservoir of larger PAHs in cold prestellar sources.

The abundance of carbon contained in PAHs has been previously estimated from the UIR band emission from different regions of the ISM. Total carbon abundances of ~14 and $\sim 60 \times 10^{-6}$ have been derived for PAHs with <100 carbon atoms in PDRs near hot stars and the diffuse ISM, respectively (*1*, *33*). Assuming that those PAHs contain an average of 50 carbon atoms, the PAH abundance in PDRs relative to H nuclei is $\gtrsim 3 \times 10^{-7}$. If the PAH population from dense molecular clouds is inherited during star formation, gas-phase pyrene could have accounted for up to ~1% of all PAHs in the presolar nebula. If the dense cloud TMC-1 has a PAH abundance similar to that of the diffuse ISM, the implication is that only a small fraction of its PAH content has been detected. Because radio observations are only sensitive to gas-phase cyanopyrene, we cannot determine the amount condensed on solid dust grains. We estimate that the abundance of solid-state pyrene locked up on dust grains is $\sim 1 \times 10^{-6}$ (relative to H nuclei), on the basis of the gas-phase abundance estimated above and its expected depletion time under TMC-1 conditions (supplementary text).

In the Solar System, comets are composed of ices and refractory material, which could reflect the composition of dust grains from the parent molecular cloud (the presolar nebula). By contrast, rocky bodies, such as asteroids, are generally depleted in carbon compared with comets (*34*). To compare our estimated solid-phase pyrene abundance to the carbon budget of comets, which are commonly reported relative to silicon, we converted the carbon abundance from being relative to H to relative to Si (supplementary text). We estimate a carbon abundance for solid-phase pyrene, relative to Si, of C/Si $\sim 0.02 \times 10^{-6}$, which is ~0.4% of the carbon budget of comets (*34*). This estimated abundance of pyrene in Solar System materials is consistent with the measured abundance in Ryugu samples, indicating inheritance from the presolar nebula to asteroids.

Pyrene formation in TMC-1

Formation of PAHs can be characterized by the temperature at which growth occurs and whether they involve bottom-up mechanisms from small precursors or top-down destruction of dust grains or larger PAHs (*35*). High-temperature bottom-up routes to PAHs include the hydrogen abstraction C_2H_2 addition (HACA) mechanism (*36*). Experiments have shown that addition of acetylene (C_2H_2) to the 4-phenanthrenyl radical ($C_{14}H_9$) can produce pyrene under high-temperature conditions, such as those found in carbon-rich circumstellar envelopes (*12*). Because this reaction has an activation energy barrier of ~20 kJ mol^{-1}, we do not expect it to operate in TMC-1 or other low-temperature environments. Alternatively, the hydrogen abstraction vinylacetylene addition (HAVA) mechanism could operate in the low-temperature conditions in dense clouds (*36*). HAVA can produce naphthalene from phenyl (*37*); however, astrochemical models of TMC-1 that include the HAVA mechanism cannot reproduce the observed abundances of 1- and 2-cyanonaphthalene (*14*), nor is the HAVA mechanism by means of 4-phenanthrenyl expected to produce pyrene (*38*).

If the pyrene present in TMC-1 is formed in circumstellar envelopes, it must survive its ejection into the diffuse ISM and subsequent incorporation into dense molecular clouds (Fig. 4). Laboratory experiments have shown that small cationic PAHs could be stabilized by fast radiative cooling, which would make them more stable in the diffuse ISM (*39*). However, the pyrene in Ryugu samples has been shown to have formed at low temperature (*10*), which is inconsistent with an origin in circumstellar envelopes.

We conclude that cyanopyrene is present in the dense molecular cloud TMC-1. We are unable to explain its abundance with previously proposed PAH formation mechanisms, so alternative pathways are required.

REFERENCES AND NOTES

1. A. Tielens, *Annu. Rev. Astron. Astrophys.* **46**, 289–337 (2008).
2. A. Léger, J. L. Puget, *Astron. Astrophys.* **137**, L5–L8 (1984).
3. L. J. Allamandola, A. G. G. M. Tielens, J. R. Barker, *Astrophys. J.* **290**, L25 (1985).
4. M. Chabot, K. Béroff, E. Dartois, T. Pino, M. Godard, *Astrophys. J.* **888**, 17 (2020).
5. E. Dwek *et al*., *Astrophys. J.* **475**, 565–579 (1997).
6. E. Habart, A. Natta, E. Krügel, *Astron. Astrophys.* **427**, 179–192 (2004).
7. M. H. Studier, R. Hayatsu, E. Anders, *Science* **149**, 1455–1459 (1965).
8. S. J. Clemett, S. A. Sandford, K. Nakamura-Messenger, F. Hörz, D. S. McKay, *Meteorit. Planet. Sci.* **45**, 701 (2010).
9. H. Naraoka *et al*., *Science* **379**, eabn9033 (2023).
10. S. S. Zeichner *et al*., *Science* **382**, 1411–1416 (2023).
11. H. Naraoka, A. Shimoyama, K. Harada, *Earth Planet. Sci. Lett.* **184**, 1–7 (2000).
12. L. Zhao *et al*., *Nat. Astron.* **2**, 413–419 (2018).
13. E. R. Micelotta, A. P. Jones, A. G. G. M. Tielens, *Astron. Astrophys.* **526**, A52 (2011).
14. B. A. McGuire *et al*., *Science* **371**, 1265–1269 (2021).
15. A. M. Burkhardt *et al*., *Astrophys. J. Lett.* **913**, L18 1(2021).
16. J. Cernicharo *et al*., *Astron. Astrophys.* **649**, L15 (2021).
17. M. L. Sita *et al*., *Astrophys. J. Lett.* **938**, L12 (2022).
18. M. Frenklach, A. W. Jasper, A. M. Mebel, *Phys. Chem. Chem. Phys.* **26**, 13034–13048 (2024).
19. M. Lecasble, L. Remusat, J.-C. Viennet, B. Laurent, S. Bernard, *Geochim. Cosmochim. Acta* **335**, 243–255 (2022).
20. J. C. Aponte *et al*., *Earth Planets Space* **75**, 28 (2023).
21. A. N. Byrne, C. Xue, I. R. Cooke, M. C. McCarthy, B. A. McGuire, *Astrophys. J.* **957**, 88 (2023).
22. B. A. McGuire *et al*., *Astrophys. J. Lett.* **900**, L10 (2020).
23. N. Balucani *et al*., *Astrophys. J.* **545**, 892–906 (2000).
24. I. R. Cooke, D. Gupta, J. P. Messinger, I. R. Sims, *Astrophys. J. Lett.* **891**, L41 (2020).
25. I. Garkusha, J. Fulara, P. J. Sarre, J. P. Maier, *J. Phys. Chem. A* **115**, 10972–10978 (2011).
26. Materials and methods are available as supplementary materials.
27. I. R. Cooke *et al*., *Astrophys. J.* **948**, 133 (2023).
28. R. A. Loomis *et al*., *Nat. Astron.* **5**, 188–196 (2021).
29. P. Gratier *et al*., *Astrophys. J. Suppl. Ser.* **225**, 25 (2016).
30. J. Cernicharo, M. Guelin, *Astron. Astrophys.* **176**, 299 (1987).
31. E. B. Jenkins, *Astrophys. J.* **700**, 1299–1348 (2009).
32. P. Pratap *et al*., *Astrophys. J.* **486**, 862–885 (1997).
33. A. Li, B. T. Draine, *Astrophys. J.* **554**, 778–802 (2001).
34. E. A. Bergin, G. A. Blake, F. Ciesla, M. M. Hirschmann, J. Li, *Proc. Natl. Acad. Sci. U.S.A.* **112**, 8965–8970 (2015).
35. H. Andrews *et al*., *Astrophys. J.* **807**, 99 (2015).
36. R. I. Kaiser, N. Hansen, *J. Phys. Chem. A* **125**, 3826–3840 (2021).
37. D. S. N. Parker *et al*., *Proc. Natl. Acad. Sci. U.S.A.* **109**, 53–58 (2012).
38. L. Zhao *et al*., *Nat. Commun.* **10**, 1510 (2019).
39. M. H. Stockett *et al*., *Nat. Commun.* **14**, 395 (2023).
40. J. Cernicharo *et al*., *Astrophys. J.* **546**, L123–L126 (2001).
41. R. Chown *et al*., *Astron. Astrophys.* **685**, A75 (2024).
42. J. Montillaud, C. Joblin, D. Toublanc, *Astron. Astrophys.* **552**, A15 (2013).
43. N. Arulanantham *et al*., *Astrophys. J. Lett.* **965**, L13 (2024).
44. G. Wenzel, I. R. Cooke, B. McGuire, GOTHAM Collaboration, Detection of interstellar 1-cyanopyrene: A four-ring polycyclic aromatic hydrocarbon, Version v1, Zenodo (2024); https://doi.org/10.5281/zenodo.12601219.

ACKNOWLEDGMENTS

We thank T. Lamberts for helpful discussions. The National Radio Astronomy Observatory is a facility of the NSF operated under cooperative agreement by Associated Universities, Inc. The Green Bank Observatory is a facility of the NSF operated under cooperative agreement by Associated Universities, Inc. **Funding:** G.W., D.A.S., and B.A.M. acknowledge support from an Arnold and Mabel Beckman Foundation Beckman Young Investigator Award. M.D., Z.T.P.F., M.S.H., and B.A.M. acknowledge support from the Schmidt Family Futures Foundation. A.M.B. was supported by the Aisiku Summer Research Fellowship. A.N.B. acknowledges support from NSF Graduate Research Fellowship grant 2141064. C.X. and B.A.M. acknowledge support of NSF grant AST-2205126. I.R.C. acknowledges support from the Natural Sciences and Engineering Research Council of Canada (grant RGPIN-2022-04684), the Canada Foundation for Innovation, and the B.C. Knowledge Development Fund. P.B.C. and M.C.M. were supported by NSF award no. AST-2307137. M.A.C. and S.B.C. were supported by the Goddard Center for Astrobiology and by the NASA Planetary Science Division Internal Scientist Funding Program through the Fundamental Laboratory Research work package. H.G. acknowledges support from the NSF as part of his independent research and development plan; any opinions, findings, and conclusions expressed in this material are those of the authors and do not necessarily reflect the views of the NSF. **Author contributions:** G.W. performed spectroscopic experiments, analyzed observational data, conducted quantum chemical calculations, and wrote the manuscript. I.R.C. analyzed observational data and wrote the manuscript. P.B.C. performed spectroscopic experiments. E.A.B. analyzed observational results. S.Z. performed the experimental synthesis. A.M.B., A.J.R., and C.X. performed radio observations. M.C.M. and A.E.W. supervised laboratory experiments. B.A.M. performed radio observations, analyzed observational data, wrote the manuscript, and designed the project. All authors commented on and revised the manuscript. **Competing interests:** The authors declare that they have no competing interests. **Data and materials availability:** The GOTHAM observations are available through the National Radio Astronomy Observatory and Green Bank Observatory archives at https://data.nrao.edu/portal/ under project codes AGBT17A_164, AGBT17A_434, AGBT18A_333, AGBT18B_007, AGBT19B_047, AGBT20A_516, AGBT21A_414, and AGBT21B_210, or at https://www.gb.nrao.edu/GbtLegacyArchive/GOTHAM/. The calibrated and reduced observational data windowed around the reported transitions; the catalog of 1-cyanopyrene transitions derived from the laboratory experiments, with their respective quantum numbers; and the partition function used in the MCMC analysis are all archived at Zenodo (*44*).

SUPPLEMENTARY MATERIALS

science.org/doi/10.1126/science.adq6391
Materials and Methods
Supplementary Text
Figs. S1 to S11
Tables S1 to S5
Movie S1
References (*45*–*62*)

Submitted 23 May 2024; accepted 10 October 2024
Published online 24 October 2024
10.1126/science.adq6391